Biointerface Research in Applied Chemistry
Platinum Open Access Journal (ISSN: 2069-5837)

Article
Volume 11, Issue 3, 2021, 10412 - 10428
https://doi.org/10.33263/BRIAC113.1041210428

Preparation and Characterization of Folate Decorated 5-Fluro Uracil Loaded Albumin Nanoparticles and *In vitro* Evaluation of its Cytotoxic Effect

Hoda Mohamed [1], Mervat Asker [1], Nahla Kotb [2], Hosam Abdelwahab [2,*]

[1] Department of Biochemistry, Faculty of Pharmacy, Zagazig University, Egypt
[2] Biologics and Innovations Sector, Egyptian Drug Authority, Egypt
* Correspondence: hosamabdelhay90@gmail.com;

Received: 28.09.2020; Revised: 22.10.2020; Accepted: 23.10.2020; Published: 26.10.2020

Abstract: In this study, a trial aims to decrease side effects and increase the efficacy of 5FU was established through active targeting of folate receptor overexpressing cancer cells using bovine serum albumin as a nanocarrier and folic acid as a targeting ligand. Physical characterization of size, potential, and polydispersity index (PDI) was performed, and (265.45 nm) particles with (- 31.1 mV) potential and (0.072) PDI were produced. For evaluation of the efficacy of the suggested formulation against the free form of the 5FU, a cytotoxic assay was performed on (Caco2, MCF7), a human colon cancer cell line, and a human breast cancer cell line, respectively, with different folate receptor-expressing features. MTT, NR & ATP assays were used, and all showed higher significant efficacy and a lower side effect of the formulation. Biochemical analysis of oxidative stress biomarker {Malonaldehyde (MDA)}, antioxidants biomarkers {Glutathione reductase (GR), Glutathione peroxidase (GPx)}, and a detoxifying enzyme {Glutathione transferase (GST)} was carried out along with quantitative real-time polymerase chain reaction (PCR) analysis of B cell lymphoma 2 (Bcl-2) gene. The results confirmed the cytotoxicity assay results. These results give new hope for using 5FU in a more effective and safe way in treatment.

Keywords: 5 FU; nanoparticles; folate decorated; albumin; cancer; cytotoxic effect.

1. Introduction

Among the different categories of chemotherapeutic agents against cancer, antimetabolites are widely used since the drug (4-amino-folic acid or aminopterin) was discovered by Faber in 1947 as the first antifolate drug to be used clinically to cause remission of leukemia successfully [1,2]. These agents can prevent cell division by being structurally resembling naturally occurring substances but, to a certain degree, to be still different enough to interfere with the natural cell biochemical metabolic pathways. This similarity enables antimetabolites either to inhibit essential enzymes during the nucleic acid synthesis pathway like what methotrexate- a folic acid antagonist- does or by substituting an essential nucleotide in the DNA or RNA strand, rendering it inactive like purine and pyrimidine antimetabolites (6 – mercaptopurine and 5 Flurouracil, respectively) [3,4].

5 Flurouracil (5FU) is a pyrimidine antimetabolite drug approved by the food and drug administration (FDA) in 1980 and synthesized by adding a Fluro atom to the 5th position on the pyrimidine ring of uracil, an essential nucleotide for RNA synthesis. It is widely used in combination with other anticancer drugs such as irinotecan and oxaliplatin in the treatment of

a variety of cancers such as colorectal, head, neck, and breast cancer [5]. Inside the cell, after being internalized, it is catabolized to fluorodeoxyuridine monophosphate (FdUMP), fluorodeoxyuridine triphosphate (FdUTP), and fluorouridine triphosphate (FUTP). These active metabolites disrupt RNA synthesis by misincorporation instead of uracil and inhibition of the action of Thymidine synthetase (TS) an essential enzyme for *de novo* synthesis pathway of thymidine nucleotide in DNA structure, exerting its cytotoxic effect by preventing DNA replication process. Many side effects were recorded for 5FU, including diarrhea, dehydration, abdominal pain, nausea, stomatitis, intestinal mucositis, and hand-foot syndrome [6]. Despite being of unclear causes, cardiovascular toxicity is reported as a side effect for 5FU [7,8].

Drug stacked nanoparticles presented an answer for taking care of such confinements so as to build the adequacy and abatement of the reactions and obstruction against 5 FU. Including cytotoxic agents inside nano-sized polymers (e.g., Chitosan, Albumin, etc.) has been tested and showed good encapsulation, efficacy, and stability [9-13]. Albumin is the most plentiful protein in plasma (35– 50 g/L human serum), which is stable in pH (4-9) and could withstand heat up to 60 ºC for 10 hours [11]. In addition to these physicochemical advantages, many other properties give the albumin types -human serum albumin (HAS) [14] or bovine serum albumin (BSA) - the chance to be a perfect candidate in drug delivery systems. The particular take-up in tumor and excited tissue, prepared accessibility, biodegradability, and absence of toxicity are examples of these recommending properties [15,16].

Active targeting of chemotherapy is one of the applications of the old dream of Paul Erlich; the Magic Bullet has been suggested in the 1900s. It aims to make new designs of the drug molecules to be delivered to diseased tissues in higher concentrations than healthy tissues, a way that increases efficacy and decreases side effects to a great extent. In active targeting, we simply attach the drug molecule - either directly or after incorporation in a carrying system – to a ligand such as an antibody or other ligands like folic acid that can recognize the diseased tissue [17,18]. Folic acid proved to be a promising targeting ligand for therapeutic or diagnostic nanoparticles in the past few years of research [19-22].

Folate receptor is also known as a high-affinity membrane-bound protein that controls the uptake of folic acid inside the cell [23]. Folate receptor and specifically the isoform alpha is found to be overexpressed on the surface of many tumors [24], which makes it a promising target to be investigated and used [25]. Folate receptor expression varies from cell line to another as it was found to be expressed in high levels on the surface of the Caco2 Cell line [25] while it was in a non-detectable level for the MCF-7 Cell line [26].

Half maximal inhibitory concentration (IC50) is a widely used measure of how effective a drug is when assayed *in vitro*, such as in cell culture assays. It means how much of the drug is required to inhibit a biological process to half [27]. Examples of a biological process that can be evaluated using such terms include some enzyme activities and cell membrane integrity [28].

In this study, a BSA nanoparticle loading 5FU was prepared then decorated with folic acid as a targeting delivery system for cancer treatment. After evaluating the formulated system (5FU-BSA-FA) by characterizing the physical properties like particle size, zeta potential, polydispersity index (PDI), and Drug Entrapment Efficacy (DEE), the system was tested for efficacy using two cell lines with different folate receptor-expressing patterns, human colon carcinoma cell line (Caco2) as a folate receptor overexpressing cell line & human breast cancer cell line (MCF7) as a negative folate receptor-expressing cell line using a complementary

testing protocol including three independent *in vitro* cytotoxicity assays {MTT, NR & ATP}. Biochemical analysis of antioxidant biomarkers {Glutathione reductase (GR), Glutathione peroxidase (GPx), a detoxifying enzyme {Glutathione transferase (GST)}, and an oxidative stress biomarker {Malonaldehyde (MDA)} as well as a quantitative real-time polymerase chain reaction (PCR) assay for an anti-apoptotic gene {B cell lymphoma 2 (Bcl-2)}.

2. Materials and Methods

2.1. Materials.

Folic acid, Phosphate buffer saline, and N-Hydroxy succinic acid, Neutral red dyes obtained from (Bio Basic, Canada). N, N Di cyclo carbodiimide, and Triethylamine obtained from (Arcos, Germany). Bovine serum albumin fraction V was provided by (LSP, USA). Fetal Bovine serum, trypsin, Antibiotic sterile solution, RPMI cell culture medium, and Trypan blue dye solution obtained from (Lonza, Switzerland). The 5FU was provided as powder, and 3-(4, 5-Dimethylthiazole-2-yl)-2, 5-diphenyltetrazolium (MTT) dyes purchased from (Sigma Aldrich, USA). Ethanol, glacial acetic acid, glutaraldehyde, acetonitrile, and dimethyl sulfoxide was used as analytic reagents were purchased as analytic agents and were of high-performance liquid chromatography grade from (Thermoficher scientific, UK). Adenosine triphosphate (ATP) assay Kit containing (ATP substrate, dilution buffer & enzyme) was provided by (Biovision, USA). Bradford protein assay kit with dye reagent (Thermo Scientific, USA). Primers of *Bcl-2*: F, 5′-TGTGGATGACTGAGTACCTGAACC-3′ and R, 5′-CAGCCAGGAGAAATCAAACAGAG-3′; *GAPDH* (housekeeping gene): F, 5′-CGTCTGCCCTATCAACTTTCG-3′ and R, 5′-CGTTTCTCAGGCTCCCTCT-3′ were synthesized by LGC Biosearch Technologies (Novato, CA, USA). Readymade kits for biochemical analysis (Biodiagnostic, Cairo, Egypt). RNeasy Mini Kit (Qiagen, Valencia, CA, USA). High-Capacity cDNA Reverse Transcription Kit (Applied Biosystems, Foster City, CA, USA). The water used was pretreated with the Milli-Q plus system (Merck Millipore, USA). Cell lines are provided from (Vacsera tissue culture unit, Egypt).

2.2. Instruments.

Biological safety cabinet class II (Thermo Scientific, HERA safe, Germany), 37±1 ºC Co_2 Incubator (Thermo Scientific, Germany), Inverted microscope (Olympus, USA), and a microplate ELISA multimode reader with Magellan data analysis software (Tecan, Austria) was used in tissue culture measurements. An Agilent-1200 HPLC (Agilent Technologies, Germany) equipped with a photodiode array (PDA) detector, auto-sampler, and temperature-controlled column compartment was used for chromatographic separations. Malvern zeta sizer Nano ZS (Malvern Instruments Ltd., UK) fitted with 4 mW helium/neon laser at 633 nm wavelength along with non-invasive back-scatter optics at a detection angle of 173º was used for Dynamic light scattering (DLS) analysis. PCR system (Applied Biosystems, USA), Thermal cycler (Applied Biosystems), and NanoDrop 2000 (Thermo Fisher Scientific, Waltham, MA, USA) was used for quantitative real-time PCR analysis. UV-Visible spectrophotometer (Shimadzu Corporation, Japan) was used for biochemical and biomarker analysis.

2.3. Methods.

2.3.1. Preparation of Folate decorated 5FU- BSA nanoparticles (5FU-BSA-FA).

Folic acid was activated to form an ester with N-hydroxysuccinimide (NHS) by the method [29]. Folic acid (1 g dissolved in 20 ml of dry dimethyl sulfoxide plus 0.5 ml of triethylamine) was reacted with NHS (0.52 g) in the presence of dicyclohexylcarbodiimide (0.94 g) overnight at room temperature. The by-product, dicyclohexylurea, was removed by filtration while the product in the filtrate, NHS-folate, was precipitated and washed several times with ice-cold anhydrous ether. The precipitate was dried under a vacuum and stored at -20 ºC as a yellow powder for later use.

For the preparation of BSA nanoparticles, we followed the desolvation technique [30]. A 2 ml solution of BSA in distilled water (100 mg/ml) was kept under continuous stirring (500 rpm) using a stirring magnet while adding a desolvating agent ethanol dropwise (1 ml/min) until milky white turbidity was obtained then 170 µl of 8% Glutaraldehyde solution was added dropwise to induce crosslinking. The stirred nanoparticles were kept overnight under continuous stirring at room temperature. The obtained nanoparticles were purified by centrifugation (12000 rpm for 20 min) and resuspension of the pellet in water by ultrasonication using a probe sonicator for not less than 5 min.

To prepare 5FU encapsulating BSA nanoparticles, the same procedure described above was used except dissolving the BSA in 2 ml (2 mg/ml) 5FU solution instead of using distilled water as a solvent; the rest of the steps, including the purification, were exactly the same.

To induce conjugation between albumin nanoparticles and the activated folate NHS ester, the reported procedure by Zhao was followed [11] 5mg/ml solution of NHS folate in carbonate- bicarbonate buffer (pH 10) was added to the nanoparticles suspension on stirring and kept overnight, then the conjugated nanoparticles were purified and dried as previously described.

2.3.2. Characterization of nanoparticles.

2.3.2.1. Particle size and zeta potential.

Particle size and zeta potential of the prepared three groups: 5FU-BSA-FA, 5FU-BSA & BSA-FA were measured by DLS after suitably diluting the sample (1:100) in purified water (MilliQ water system) [31].

2.3.2.2. NHS Folate preparation efficiency.

Both Folic acid powder and NHS-Folate prepared powder were scanned using a UV spectrophotometer in the range of 250 to 400 nm to be tested for matching [11].

2.3.2.3. Drug entrapment efficacy.

5FU was quantified using a previously reported reversed-phase high-performance liquid chromatography (RP-HPLC) method, as previously reported [32]. All separations were carried out using Zorbax 300-C18 column (250mm ×4.6 mm) particle size 5µm and pore size 250 A°, operated at flow rate 1 mL/min using a mobile phase consisted of distilled water and acetonitrile in ratio 70:30 % V/V in an isocratic mode. The injection volume was 20 µl through

an automated injector, and the conditions were kept under room temperature, and UV detection using a PDA detector was performed at 227 nm.

A standard calibration curve was established using known concentrations of 5FU, then the concentration of 5FU in the supernatant purification cycle was determined. Drug entrapment efficacy was calculated using the following equation:

$$\text{DEE} = \frac{\text{5 FU added amount (total)} - \text{5 FU amount in supernatant} \times 100}{\text{5FU added amount (total)}}$$

2.3.3. *In vitro* cell cytotoxicity assay.

For *in vitro* evaluation of the cytotoxicity of the prepared formulations, (Caco2&MCF7) colon and breast cancer, cell lines were used. Cell lines were grown and maintained using RPMI growth media containing 10% FBS and 1% antibiotic and 1% L-Glutamine sterile solutions in 37 ºC in 5% CO_2 incubator and detached then subcultured when required using Trypsin solution with EDTA.

2.3.3.1. MTT assay.

Cell cytotoxicity assay was carried out by seeding cells (Caco2 & MCF7 separately) in 96 well cell culture plates with a density of $1x10^4$ (Cells/well) counted by Hemocytometer technique [33] and using 10% growth RPMI medium as diluent then incubated overnight in 5% CO_2, 37 ºC to attach.

Afterward, the media was discarded and replaced with a serial concentration of the drug in three formulations (Free 5 FU, 5 FU-BSA & 5 FU-BSA- FA) ranged from (167 – 2 µg/ml) using the same growth medium as a diluent. Every concentration was assayed in triplicate, keeping wells without any drug added only growth media as a control group, then the plate was incubated in the same conditions for 48 hours. MTT assay procedure was followed as described [34]. Briefly, the supernatant above the cells was discarded, and 20 µl of (5 mg/ml) MTT solution in PBS was added to each well. After 2-4 hours of incubation at 37 ºC, MTT was discarded, and 150 µl of DMSO was added to each well then incubated again for 30 min till complete dissolving of formazan crystals. Then absorbance was measured at 570 nm, and cell viability was represented as a percent of a control group. Then, cells viability against concentration was plotted to calculate IC50 of 5 FU in different forms for each cell line.

2.3.3.2. Neutral red uptake assay.

In the neutral red assay, Caco2 & MCF7 cells were seeded separately, and two different formulations of the drug (Free 5 FU, 5FU-BSA-FA) were tested in the same way as in the MTT assay. The neutral red dye was prepared a day before in the concentration of 40 µg/ml using the same used cell growth medium as a diluent and kept at 37 ºC till use the next day. After the 48 hours period of incubation of cells and drug formulations, the medium was discarded. Then 100 µl of the dye was added to all wells and incubated at 37 ºC for at least two hours. After incubation, the dye was discarded, and 150 µl of destaining solution (1% Glacial acetic acid,49% Ethanol & 50% distilled water) was added to all wells until completely dissolving of the retained dye. Then the absorbance was measured at 540 nm, and cell viability was represented as a percent of a control group [35].

2.3.3.3. ATP luminescent assay.

Caco2 & MCF7 cells were seeded separately, and two different formulations of the drug (Free 5 FU, 5FU-BSA-FA) were tested in the same way as in MTT and Neutral red assays noticing that the type of the 96 wells plate is different as it has to be opaque to be suitable for this type of luminescence assay. After 24 hours of incubation, the medium was discarded, and a new growth medium containing different concentrations of the drug of the Free 5 FU, 5 FU-BSA- FA was added to flasks. After 48 hours of incubation, the cells were assayed for viability using ATP assay kit,10 µl of cell suspension was added in the well of 96wells opaque cell culture plate, then 100 µl of nucleotide buffer was added to each well, then 10 µl of the ATP monitoring solution was added to each well then luminescence was measured immediately using multimode reader and viability was calculated as a percentage of the control group [36].

2.3.4. RNA isolation and cDNA synthesis.

Caco2 & MCF7 cells were treated with IC50 of the two different formulations of the drug (Free 5 FU, 5FU-BSA-FA) and incubated for 24 hours at 37°C in a humidified CO_2 incubator. Total cellular RNA was extracted from the untreated (control) and treated cells using the RNeasy Mini Kit. The concentration and purity of the isolated RNA were performed by using NanoDrop 2000. High-Capacity cDNA Reverse Transcription Kit was used for DNA synthesis. 20 µl reaction mixture was used containing 12 µl of total RNA (1 µg), 2 µL 10× RT random primers, 1 µL 10× dNTP Mix, 1 µL RNase inhibitor, 1 µL MultiScribe Reverse Transcriptase, and 3 µL nuclease-free water. Thermal cycler was used for performing reverse transcription and adjusted for 10 minutes at 30 °C, for 50 minutes at 42 °C and 5 minutes at 95 ºC then cooled at 4 °C for 5 min [37].

2.3.5. Quantitative real-time-PCR.

The expression of the target gene (bcl-2) was quantified using SYBR Green real-time PCR on cDNA extracted from Caco2 & MCF7 cells. PCR system was used, and each PCR amplification reaction was performed in 20 µl reaction mixture containing 10 µL Power SYBR Green PCR Master Mix (2x), 2 µl cDNA sample (100 ng), 1 µL forward primer (10 µM), 1 µL reverse primer (10 µM), and 6 µL double-distilled water. The gene expression was calculated using a comparative threshold cycle (Ct) where $\Delta\Delta C_T$ = [C_T target gene–C_T*GAPDH*] (treated sample) –[C_T target gene–C_T *GAPDH*](untreated sample). The relative gene expression was calculated using $2^{-\Delta\Delta C_T}$ method [37].

2.3.6. Biochemical analysis.

Caco2 & MCF7 cells were treated with the IC_{50} values of the two different formulations of the drug (Free 5 FU, 5FU-BSA-FA) for 24 hours and incubated at 37°C. Cells were harvested, washed twice with PBS, and centrifuged at 2,000 ×*g* for 5 minutes. The obtained pellets were resuspended in PBS, followed by cold sonication and then centrifugation at 4,000 ×*g* for 15 minutes. The supernatants were then collected and assayed for determining the levels of GR, GPx, and GST along with MDA level using readymade kits and UV-Visible spectrophotometer according to the manufacturer's manual by biodiagnostic. The total protein was determined in cells by the Bradford method [38,39], and the activity levels of antioxidant enzymes and MDA were calculated per mg protein.

2.3.7. Statistical analysis.

To confirm the results and to ensure the significance of the cytotoxicity assay for MTT, Neutral red and ATP assay of CaCo2 & MCF7 cell lines, PCR, and biochemical analysis, the P-value was calculated by comparing different groups using One way ANOVA or unpaired t-student test and the difference was considered statistically significant at $P < 0.05$. Moreover, IC50 was undertaken, and all statistical analysis was performed using Graphpad prism7 software (Graphpad Software, La Jolla, CA.USA).

3. Results and Discussion

3.1. Characterization of nanoparticles.

3.1.1. Particle size and zeta potential.

The formulations (5FU-BSA-FA, 5FU-BSA, BSA-FA) were prepared using the desolvation technique, which results in the synthesis of a uniform BSA nanoparticle. Glutaraldehyde alone -without using carboxymethyl beta-cyclodextrin- as a cross-linker was used, which forms a stable aldehyde bond between molecules and prevent the release of the drug while delivering of the nanoparticles to tumor cells. By applying this procedure of nanoparticle synthesis and upon the physical characterization of the three prepared formulations (5FU-BSA-FA, 5FU-BSA, BSA-FA), which includes measuring particle size and zeta potential and PDI, it was found that all results are aligned with previous preparations using the same desolvation technique [11]. The mean of particle size and zeta potential expressed as a standard of deviation of three independent readings and the PDI of the three formulations, as shown in Fig. 1 and summarized in Table1.

Table 1. Summary of particle size, zeta potential, and PDI of the studied formulations.

	Particle size (nm)	PI	Zeta potential (mV)
5FU-BSA-FA	265.45	0.072	- 31.1
5FU-BSA	245.8	0.122	- 29.4
BSA-FA	219.05	0.045	-26.75

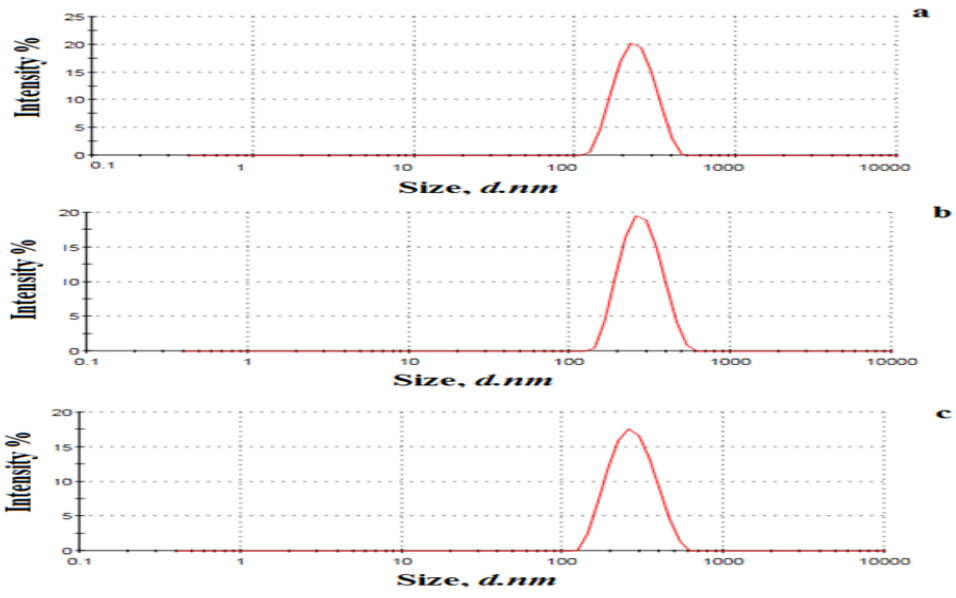

Figure 1. Intensity size distribution of: **(a)** 5FU, **(b)** 5FU-BSA, **(c)** 5FU-BSA-FA, showing the monomer peak of 5FU ,5FU-BSA ,5FU-BSA-FA respectively.

3.1.2. Folic acid conjugation efficiency.

Successful formulation of NHS-Folate was confirmed by scanning (5 mg/ml) solution samples of both folic acid and NHS-Folate using UV spectrometer within range (250-400 nm), and both showed maximum absorption peak on (366 nm) [43] matched spectrum of Folic acid, NHS-Folate, and FA-Naked Nanoparticles are shown in Fig. 2.

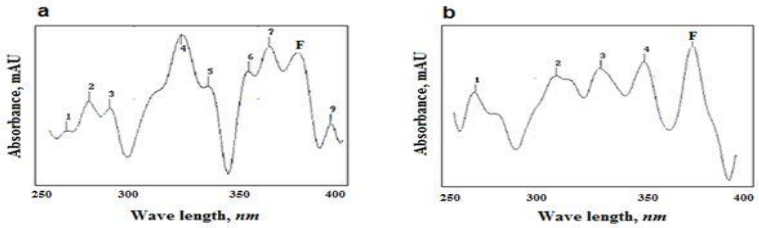

Figure 2. UV spectrum of **(a)** NHS Folate, **(b)** Folic Acid standard solution showing peak F: A matching peak of 366 nm.

3.1.3. Drug entrapment efficacy.

The drug entrapment efficacy of the formulations was calculated using the RP-HPLC system. First, a standard calibration curve of 5FU was performed using a concentration range (5-1000 µg/ml); a linear relationship with a correlation coefficient (r=0.999) was obtained. The concentration of drug in supernatant that collected from the purification of the formulation by centrifugation was determined by measuring its area under peak as a mean of three independent injections of the sample than using the standard curve to define the corresponding concentration (Fig. 3), and the concentration of the supernatant of the drug DEE are calculated and summarized in Table 2.

Table 2. Summary of the supernatant concentrations and the entrapped drug percentage in the studied formulations.

	5FU concentration in the supernatant (µg/ml)	**DEE (%)**
5FU-BSA	52.6	82.8
5FU-BSA-FA	58.8	80.1

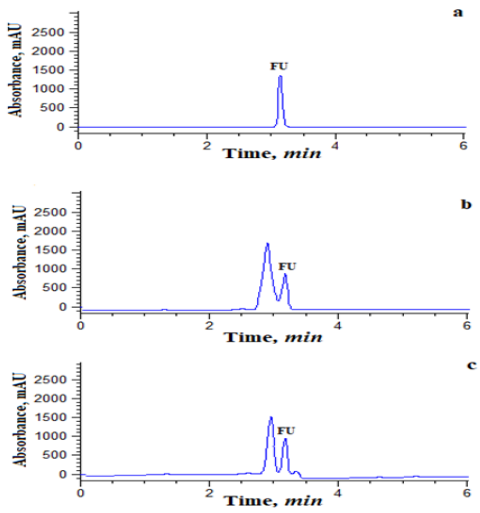

Figure 3. RP-HPLC analysis results of **(a)** 5-fu drug standard (100mg/ml), **(b)** 5 FU-BSA **(c)** 5FU-BSA-FA, showing the monomer peak of 5FU. The analysis was carried out using the Zobrax 300-C18 column; the mobile phase consists of distilled water and acetonitrile in ratio 70:30%v/v, the flow rate of 1mL/min, and detection wavelength of 227.0 nm.

3.2. In vitro cytotoxicity.

3.2.1. MTT assay.

3.2.1.1. MTT assay on the Caco2 cell line.

Knowing that cell viability and inhibitory effect assayed by MTT depends on the activity of the viable cell mitochondrial dehydrogenase enzyme to convert the yellow MTT dye to violet formazan crystals that can be dissolved and assayed for color intensity [44], the inhibitory effect of the naked BSA-FA as shown in (Fig. 4a) was minimal over the concentrations lower than 2 mg/ml of nanoparticles. This minimal inhibitory effect at the concentration of 2 mg/ml may be referred to as the cytotoxic effect of the used glutaraldehyde, and it seemed to be negligible [45]. Despite that, when 5 FU is encapsulated in the decorated nanoparticles, a significant inhibitory effect can be seen over increasing concentrations. The significance of P-value <0.05 can be statistically noticed by applying a one-way ANOVA model when comparing the corresponding concentration of 5 FU but in different forms (Free drug, 5 FU-BSA, and 5FU-BSA-FA). It was found that the folate decorated form significantly shows the more inhibitory effect (Fig. 4b). Also, the Folic acid decorated form of 5FU showed a lower IC50 value in comparison with the free form of 5FU as shown in Table 3.

Table 3. IC50 µg/mL of 5FU, 5FU-BSA-FA according to the three cytotoxic assays MTT, Neutral red, and ATP.

	Caco2 cell line			**MCF7 cell line**		
	MTT	Neutral red	ATP	MTT	Neutral red	ATP
5FU	361.2	203.9	193.2	44.66	163	156.7
5FU-BSA-FA	89.53	118	139.9	193.4	383.7	258.1

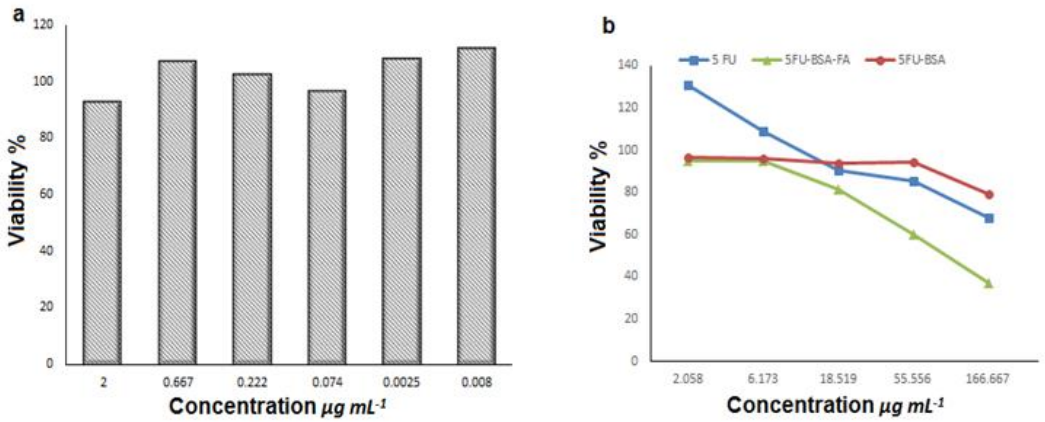

Figure 4. MTT assay results of **(a)** control group BSA-FA **(b)** 5FU, 5FU-BSA-FA, 5FU-BSA showing a significant inhibitory effect of the folic decorated form of the nanoparticle encapsulated formulations 5FU-BSA-FA.

In addition, by evaluating the linearity of the three groups, it was found that the 5FU-BSA group showed the worst linearity (r=0.65) while 5FU and 5FU-BSA-FA showed a correlation coefficient of 0.96, 0.91, respectively. This may be explained by the fact that the passive targeting effect of the nanoparticles encapsulating cytotoxic agent without being linked to an actively targeting ligand is better tested *in vivo* because it depends on the physical properties of the complete solid tumor and its microenvironment, such as the enhanced permeability and retention effect (EPR) [46].

3.2.1.2. MTT assay on the MCF-7 cell line.

In contrast, when comparing the MTT assayed the cytotoxic effect of the different concentrations of the free 5FU and the folic decorated nanoparticle on a folate receptor lacking MCF7 Cell line, using an unpaired t-student test model with adjusted P-value (< 0.05), it was found that the drug has a significantly higher inhibitory effect with a lower IC50 value than the folate decorated nanoparticles (Fig 5a). These results confirmed the role of the folate ligand in the active targeting of the prepared formulation allowing the greater extent of uptake of the cytotoxic agents by the folate receptor, which is overexpressed on the surface of the majority of solid tumor, giving a promising indicator of being an effective system for delivering the 5FU cytotoxic agent into a folate receptor overexpressing tumors more than normally folate receptor-expressing cells [47,48]. This is confirmed by the significant decrease of cell viability in the case of the Caco2 cell line when compared to the MCF7 cell line over the same concentration range of the folic acid decorated formulation (Fig. 5b).

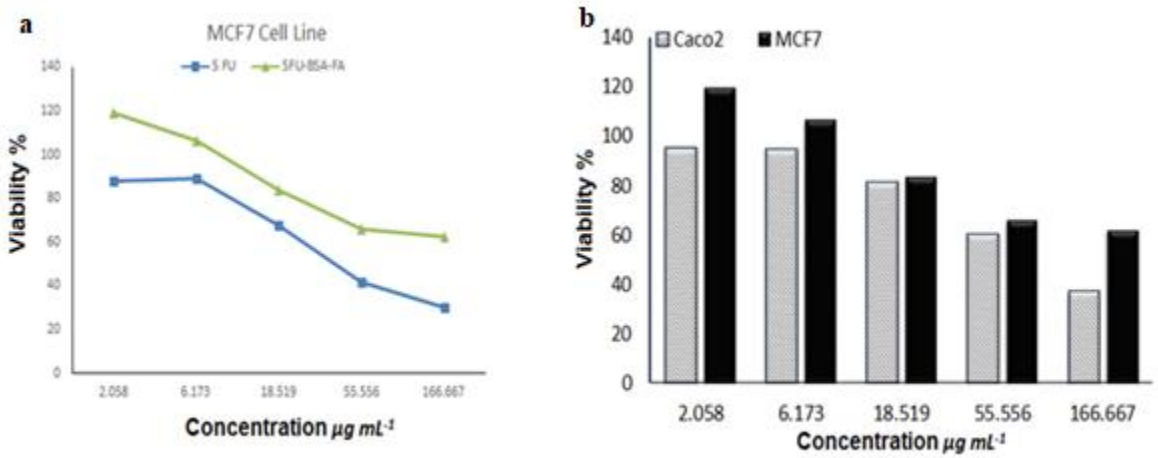

Figure 5. MTT assay results of **(a)** inhibitory effect of 5FU, 5FU-BSA-FA on MCF7 cell line, **(b)** inhibitory effect 0f 5FU-BSA-FA on Caco2 and MCF7 cell lines, showing the targeting of the 5FU into a folate receptor overexpressing Caco2 cancer cells more than negatively expressing folate receptor MCF7 cancer cells.

3.2.2. Neutral red assay.

3.2.2.1. Neutral red assay on the Caco2 cell line.

Further verification for the results of MTT assay has been confirmed through the neutral red assay method, which depends on another principle rather than the viable cell activity evaluation; in this assay, we depended on the integrity of the viable cell membrane using the neutral red dye which tends to be retained by the viable cell rather than the dead. As a result, viable cells appear in a red color, which is directly proportional to the cell count, while the dead lose the dye easily by distaining [35].

The results of the neutral red assay agreed with those of the MTT assay, as shown in Fig. 6a. The folate decorated form of the drug showed a significantly higher inhibitory effect over increasing the concentration more than that shown by the corresponding concentrations of the free form of the drug. This significance could be statistically noticed when using an unpaired t-student test model with an adjusted P-value (< 0.05). In addition, the IC50 of Folic acid decorated form of 5FU showed a lower value when compared with the value of the free form of the drug, as shown in Table 3.

3.2.2.2. Neutral red assay on the MCF7 cell line.

Cytotoxicity assay using neutral red resulted in dose-dependent growth inhibition of MCF-7 cells. However, both forms of the drug (5FU and FA-5FU BSA NPs) showed inhibition of cell viability, the free form of the drug showed a significantly higher inhibitory effect, and a lower IC50 value (Table 3) than the folate decorated nanoparticles (Fig. 6b) and that significance was proven statistically using unpaired t-student test model with adjusted P-value (< 0.05). These results also confirmed the role of the folate decorated nanoparticles form of drug as a drug carrier system to deliver drugs into the cells with an overexpressing folate receptor (Caco2) rather than the negative folate receptor-expressing cell line (MCF7).

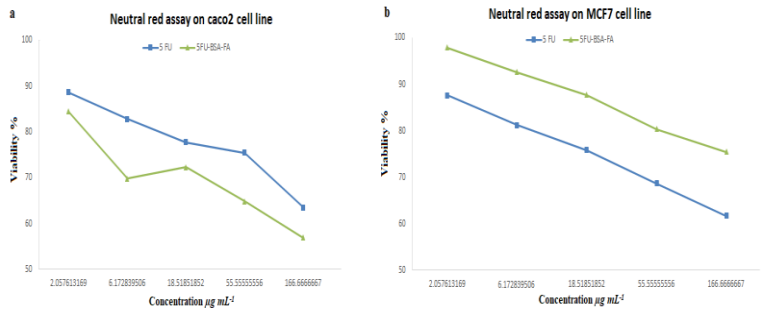

Figure 6. Results of the neutral red assay: **(a)** 5FU, 5FU-BSA-FA on caco2 cell line **(b)** 5FU, 5FU-BSA-FA on MCF7 cell line, showing a significant inhibitory effect of the folic decorated form of the nanoparticles encapsulated formulations 5FU-BSA-FA.

3.2.3. ATP luminescent assay.

3.2.3.1. ATP assay on the Caco2 cell line.

In an additional trial to validate and confirm the results of the two previous methods, the ATP assay was carried out. This assay depends on the fact that the apoptotic cell or dead cell shows decreased levels of ATP than that shown in the proliferated viable cell. Thus measuring the ATP level could be used as a successful rapid method of viability assay [36]. Fig. 7a indicates the performed comparison between the free form of 5FU and the folate decorated BSA nanoparticles form, which showed a significantly higher inhibitory effect for the folate form as ensured by using the unpaired t-student test with the same adjusted P-value (< 0.05) and a lower IC50 values as shown in Table 3.

3.2.3.2. ATP assay on the MCF7 cell line.

The ATP assay emphasized that the ability for folate decoration technique to decrease 5FU side effects could be confirmed through another way rather than MTT and neutral red. The free form of 5FU resulted in a more depletion in cell number as a consequence of cell cycle arrest, with significant higher cytotoxic effects than the folate decorated nanoparticles using the ATP assay (Fig. 7b), and that significance is statistically proven by the model of unpaired t-student test with the same adjusted P-value (< 0.05).

The concentration-dependent reduction in cell viability of MCF7 cells that was proved using both MTT and neutral red assays was further confirmed using ATP assay through an IC50 with a lower value of the free drug form than that of the folate decorated nanoparticles (Table 3).

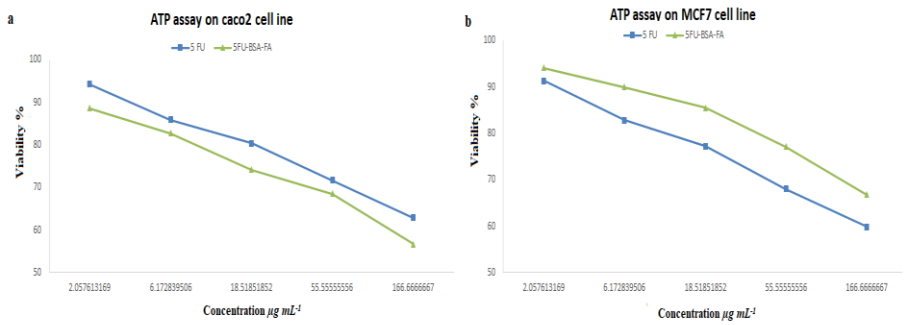

Figure 7. Results of ATP assay: **(a)** 5FU, 5FU-BSA-FA on Caco2 cell line; **(b)** 5FU, 5FU-BSA-FA on MCF7 cell line, showing a significant inhibitory effect of the folic decorated form of the nanoparticles encapsulated formulations 5FU-BSA-FA.

3.3. Quantitative real-time PCR.

Bcl-2 is a potent inhibitor of apoptotic cell death by maintaining mitochondrial membrane potential and regulating the redistribution of cytochrome c, which is a necessary cofactor for the activation of apoptotic effector proteases known as caspases [49]. Thus bcl-2 is classified as anti-apoptotic as a result of preventing the efflux of cytochrome c from the mitochondria and inhibiting the initiation of apoptosis [50]. A high level of Bcl-2 protein ensures the survival advantage to the clonal population and promotes tumorigenesis; however, 5FU was reported to cause down-regulation for bcl-2 levels in cancer cells, and this inhibitory effect plays an important role in inducing apoptosis [51].

Caco2 and Mcf7 cell lines were subjected to 24 hours treatment of the IC50 of both 5FU and 5FU-BSA-FA, and levels of bcl-2 activity were then assayed. Results showed that bcl-2 relative expression level was significantly inhibited by both the free form of the drug and the folic decorated one (P-value < 0.05). This down-regulation of Bcl-2 mRNA levels revealed that the selected gene had exhibited an important role in apoptosis induction in the studied cell lines. Moreover, the results showed a significant (P-value < 0.05) higher inhibitory effect of bcl-2 expression level in the Caco2 cell line when treated with 5FU-BSA-FA compared to those treated with the free form of the drug. On the other hand, this inhibitory effect was higher in the case of the free form of the drug compared to that of the folic decorated one when the negative folate receptor-expressing cell line (Mcf7) was treated with them (Fig. 8). These results confirmed the role of folic decoration in active targeting in the case of overexpressed folate receptor cell lines.

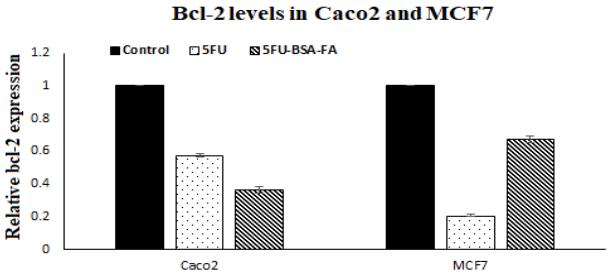

Figure 8. Effect of IC50 of 5FU and 5FU-BSA-FA on bcl-2 gene in Caco2 and MCF7 cell lines, results showed a significant inhibitory effect for both the free form drug and the folic decorated form relative to the control while the inhibitory effect of the 5FU-BSA-FA is significantly higher than that of 5FU in Caco2 and vice versa in case of MCF7. Statistical significance is expressed as $p<0.05$.

3.4. Biochemical analysis.

Oxidative stress is a case of imbalance in which an increase of the reactive oxygen species (ROS) or decrease in their removal enzyme system inside the cell takes place, which negatively affects the cell by causing degeneration, aging, and death. Therefore oxidative stress markers have long been implicated in cancer development and progression study. MDA the end product of lipid peroxidation, is commonly used as a marker of oxidative stress. However, the enzymatic systems involved in the maintenance of the intracellular redox balance can also be used as markers of the antioxidant defense systems [52].

Glutathione is a tripeptide that is found in all mammalian cells in the reduced form (GSH) and functions as an important antioxidant that serves side by side with a bunch of enzymes in removing harmful oxidative species such as oxygen superoxide and hydrogen peroxide [53]. GPx enzyme is one of these antioxidant enzymes that use GSH to remove hydrogen peroxide from the cell by reducing and causing GSH to be oxidized to Glutathione oxidized form (GSSG). Here comes the function of a second antioxidant enzyme called GR, which helps in recycling GSSG to GSH again to be reused in further antioxidant activities inside the cell [54]. Therefore, decreased levels of these enzymes indicate that the cell undergoes a high oxidative stress manner, which may lead finally to its death. On the other hand, GST is an important enzyme involved in the detoxification of many xenobiotics inside the cell. GST was reported to be downregulated in the case of cancer cells treated with 5FU, so its decrease could be a marker for the successful incorporation and effect of 5FU inside the cell [55]. Other reports suggest that the administration of 5FU causes depletion of the antioxidant enzyme activities such GPx as well as an increase in the MDA level [56,57].

Our results showed a significant increase (p-value <0.05) in MDA levels for both caco2 and mcf7 cell lines when treated with the IC50 of 5FU and 5FU-BSA-FA independently for 24 hours when compared to the control cell lines. Additionally, levels of GR, GST, GPX were significantly decreased (p-value <0.05) when the studied cell lines were treated with both the free drug and the folate decorated formulation (Table 4).

The results of the 5FU-BSA-FA formulation were significantly higher in MDA levels (p-value <0.05) and significantly lower in the levels of the antioxidant enzyme (p-value <0.05), when compared to the free drug in the case of the Caco2 cell line.

It was also shown that 5FU-BSA-FA exhibited a significantly lower MDA level (p-value <0.05) and a significantly higher (p-value <0.05) in the levels of the antioxidant enzyme when compared to the 5FU in the case of the MCF7 cell line.

Table 4. Effect of IC50 µg/mL of 5FU, 5FU-BSA-FA on levels of MDA, antioxidant enzymes & detoxifying enzyme.

	Caco2 cell line				**MCF7 cell line**			
	MDA (nmol)	**GR (mU)**	**GST (mU)**	**GPx (mU)**	**MDA (nmol)**	**GR (mU)**	**GST (mU)**	**GPx (mU)**
Control	5.69±0.12	9.34±0.12	4.65±0.65	5.29±0.46	5.15±0.16	9.55±0.09	4.75±0.17	5.42±0.06
5FU	9.48±0.29	6.36±0.12	3.23±0.59	3.37±0.22	10.47±0.57	5.63±0.19	2.37±0.39	3.27±0.38
5FU-BSA-FA	13.15±0.26	3.09±0.12	1.72±0.87	2.19±0.32	7.18±0.77	7.18±0.83	3.51±0.54	4.35±0.14

All values are expressed as mean ± SD.
All results showed a significant difference at p-value > 0.05.

4. Conclusions

Depending on the fact that folate receptors are overexpressed on the surface of many cancer types, careful preparation and evaluation of an active targeting system for delivering 5FU cytotoxic agents to cancer cells rather than the healthy by using folic acid as a ligand were carried out through this study. It was proved that through the desolvation technique, we could effectively prepare a folic decorated BSA nanoparticle incorporating 5FU cytotoxic agents inside it. That was confirmed through characterizing size, zeta potential, and entrapment efficacy. Then the efficacy of the suggested formulation was tested against the free form of the drug *in vitro* using CaCo2 & MCF7 cell lines showing the significant difference that was confirmed through a complementary testing protocol including different approaches of the assay (MTT, Neutral red & ATP) as cell viability assays. GR, GPx, GST, and MDA as a biochemical biomarker and bcl-2 real-time PCR as genetic biomarker assay. This study recommends that this 5FU-BSA-FA form may be helpful if studied clinically, aiming to increase the effectiveness and decrease side effects of 5FU, which gives new hopes to fight against cancer.

Funding

This research received no external funding.

Acknowledgments

This research has no acknowledgment.

Conflicts of Interest

The authors declare no conflict of interest.

References

1. Kaye, S.B. New antimetabolites in cancer chemotherapy and their clinical impact. *British journal of cancer* **1998**, *78*, 1-7, https://www.doi.org/10.1038/bjc.1998.747.
2. McGuire, J.J. Anticancer antifolates: current status and future directions. *Current pharmaceutical design* **2003**, *9*, 2593-2613, https://www.doi.org/10.2174/1381612033453712.
3. Peters, G.; Van der Wilt, C.; Van Moorsel, C.; Kroep, J.; Bergman, A.; Ackland, S. Basis for effective combination cancer chemotherapy with antimetabolites. *Pharmacology & therapeutics* **2000**, *87*, 227-253, https://doi.org/10.1016/S0163-7258(00)00086-3.
4. Thalambedu, N.; Khan, Y. Fluorouracil (5-FU)-induced Cardiomyopathy. *Cureus* **2019**, *11*, https://www.doi.org/10.7759/cureus.5162.
5. Vodenkova, S.; Buchler, T.; Cervena, K.; Veskrnova, V.; Vodicka, P.; Vymetalkova, V. 5-fluorouracil and other fluoropyrimidines in colorectal cancer: Past, present and future. *Pharmacology & therapeutics* **2020**, *206*, https://www.doi.org/10.1016/j.pharmthera.2019.107447.
6. Costa, D.V.; Bon-Frauches, A.C.; Silva, A.M.; Lima-Júnior, R.C.; Martins, C.S.; Leitão, R.F.; Freitas, G.B.; Castelucci, P.; Bolick, D.T.; Guerrant, R.L. 5-fluorouracil induces enteric neuron death and glial activation during intestinal mucositis via a S100B-RAGE-NFκB-dependent pathway. *Scientific reports* **2019**, *9*, 1-14, https://www.doi.org/10.1038/s41598-018-36878-z.
7. Longley, D.B.; Harkin, D.P.; Johnston, P.G. 5-fluorouracil: mechanisms of action and clinical strategies. *Nature reviews cancer* **2003**, *3*, 330-338, https://www.doi.org/10.1038/nrc1074.
8. Focaccetti, C.; Bruno, A.; Magnani, E.; Bartolini, D.; Principi, E.; Dallaglio, K.; Bucci, E.O.; Finzi, G.; Sessa, F.; Noonan, D.M. Effects of 5-fluorouracil on morphology, cell cycle, proliferation, apoptosis, autophagy and ROS production in endothelial cells and cardiomyocytes. *PloS one* **2015**, *10*, https://www.doi.org/10.1371/journal.pone.0115686.
9. Tummala, S.; Kumar, M.S.; Prakash, A. Formulation and characterization of 5-Fluorouracil enteric coated nanoparticles for sustained and localized release in treating colorectal cancer. *Saudi Pharmaceutical Journal* **2015**, *23*, 308-314, https://www.doi.org/10.1016/j.jsps.2014.11.010.

10. Sun, L.; Chen, Y.; Zhou, Y.; Guo, D.; Fan, Y.; Guo, F.; Zheng, Y.; Chen, W. Preparation of 5-fluorouracil-loaded chitosan nanoparticles and study of the sustained release in vitro and in vivo. *asian journal of pharmaceutical sciences* **2017**, *12*, 418-423, https://www.doi.org/10.1016/j.ajps.2017.04.002.
11. Zhao, D.; Zhao, X.; Zu, Y.; Li, J.; Zhang, Y.; Jiang, R.; Zhang, Z. Preparation, characterization, and in vitro targeted delivery of folate-decorated paclitaxel-loaded bovine serum albumin nanoparticles. *International journal of nanomedicine* **2010**, *5*, https://www.doi.org/10.2147/ijn.s12918.
12. Jin, K.-T.; Lu, Z.-B.; Chen, J.-Y.; Liu, Y.-Y.; Lan, H.-R.; Dong, H.-Y.; Yang, F.; Zhao, Y.-Y.; Chen, X.-Y. Recent Trends in Nanocarrier-Based Targeted Chemotherapy: Selective Delivery of Anticancer Drugs for Effective Lung, Colon, Cervical, and Breast Cancer Treatment. *Journal of Nanomaterials* **2020**, *2020*, https://www.doi.org/10.1155/2020/9184284.
13. Yoncheva, K.; Tzankov, B.; Yordanov, Y.; Spassova, I.; Kovacheva, D.; Frosini, M.; Valoti, M.; Tzankova, V. Encapsulation of doxorubicin in chitosan-alginate nanoparticles improves its stability and cytotoxicity in resistant lymphoma L5178 MDR cells. *Journal of Drug Delivery Science and Technology* **2020**, *59*, https://www.doi.org/10.1016/j.jddst.2020.101870.
14. Ghosh, P.; Roy, A.S.; Chaudhury, S.; Jana, S.K.; Chaudhury, K.; Dasgupta, S. Preparation of albumin based nanoparticles for delivery of fisetin and evaluation of its cytotoxic activity. *International journal of biological macromolecules* **2016**, *86*, 408-417, https://www.doi.org/10.1016/j.ijbiomac.2016.01.082.
15. Elzoghby, A.O.; Samy, W.M.; Elgindy, N.A. Albumin-based nanoparticles as potential controlled release drug delivery systems. *Journal of controlled release* **2012**, *157*, 168-182, https://www.doi.org/10.1016/j.jconrel.2011.07.031.
16. Jahanshahi, M.; Babaei, Z. Protein nanoparticle: a unique system as drug delivery vehicles. *African Journal of Biotechnology* **2008**, *7*.
17. Bertrand, N.; Wu, J.; Xu, X.; Kamaly, N.; Farokhzad, O.C. Cancer nanotechnology: the impact of passive and active targeting in the era of modern cancer biology. *Advanced drug delivery reviews* **2014**, *66*, 2-25, https://www.doi.org/10.1016/j.addr.2013.11.009.
18. Anarjan, F.S. Active targeting drug delivery nanocarriers: Ligands. *Nano-Structures & Nano-Objects* **2019**, *19*, https://www.doi.org/10.1016/j.nanoso.2019.100370.
19. Gazzano, E.; Rolando, B.; Chegaev, K.; Salaroglio, I.C.; Kopecka, J.; Pedrini, I.; Saponara, S.; Sorge, M.; Buondonno, I.; Stella, B. Folate-targeted liposomal nitrooxy-doxorubicin: An effective tool against P-glycoprotein-positive and folate receptor-positive tumors. *Journal of controlled release* **2018**, *270*, 37-52, https://www.doi.org/10.1016/j.jconrel.2017.11.042.
20. Li, L.; Yang, Q.; Zhou, Z.; Zhong, J.; Huang, Y. Doxorubicin-loaded, charge reversible, folate modified HPMA copolymer conjugates for active cancer cell targeting. *Biomaterials* **2014**, *35*, 5171-5187, https://www.doi.org/10.1016/j.biomaterials.2014.03.027.
21. Pan, J.; Feng, S.-S. Targeted delivery of paclitaxel using folate-decorated poly (lactide)–vitamin E TPGS nanoparticles. *Biomaterials* **2008**, *29*, 2663-2672, https://www.doi.org/10.1016/j.biomaterials.2008.02.020.
22. Vasir, J.K.; Labhasetwar, V. Targeted drug delivery in cancer therapy. *Technology in cancer research & treatment* **2005**, *4*, 363-374, https://www.doi.org/10.1177/153303460500400405.
23. Zagorac, I.; Lončar, B.; Dmitrović, B.; Kralik, K.; Kovačević, A. Correlation of folate receptor alpha expression with clinicopathological parameters and outcome in triple negative breast cancer. *Annals of Diagnostic Pathology* **2020**, *48*, https://www.doi.org/10.1016/j.anndiagpath.2020.151596.
24. Khan, M.A.; Zafaryab, M.; Mehdi, S.H.; Quadri, J.; Rizvi, M.M.A. Characterization and carboplatin loaded chitosan nanoparticles for the chemotherapy against breast cancer in vitro studies. *International journal of biological macromolecules* **2017**, *97*, 115-122, https://www.doi.org/10.1016/j.ijbiomac.2016.12.090.
25. Roger, E.; Kalscheuer, S.; Kirtane, A.; Guru, B.R.; Grill, A.E.; Whittum-Hudson, J.; Panyam, J. Folic acid functionalized nanoparticles for enhanced oral drug delivery. *Molecular pharmaceutics* **2012**, *9*, 2103-2110, https://www.doi.org/10.1021/mp2005388.
26. Sonvinco, F.; Dubernet, C.; Marsaud, V.; Appel, M.; Chacun, H.; Stella, B.; Renoir, M.; Colombo, P.; Couvreur, P. Establishment of an in vitro model expressing the folate receptor for the investigation of targeted delivery systems. *Journal of drug delivery science and technology* **2005**, *15*, 407-410, https://www.doi.org/10.1016/S1773-2247(05)50080-7.
27. Veiga, A.; Maria da Graça, T.T.; Rossa, L.S.; Mengarda, M.; Stofella, N.C.; Oliveira, L.J.; Gonçalves, A.G.; Murakami, F.S. Colorimetric microdilution assay: validation of a standard method for determination of MIC, IC50%, and IC90% of antimicrobial compounds. *Journal of microbiological methods* **2019**, *162*, 50-61, https://www.doi.org/10.1016/j.mimet.2019.05.003.
28. Aykul, S.; Martinez-Hackert, E. Determination of half-maximal inhibitory concentration using biosensor-based protein interaction analysis. *Analytical biochemistry* **2016**, *508*, 97-103, https://www.doi.org/10.1016/j.ab.2016.06.025.
29. Sun, Y.; Zhao, Y.; Teng, S.; Hao, F.; Zhang, H.; Meng, F.; Zhao, X.; Zheng, X.; Bi, Y.; Yao, Y. Folic acid receptor-targeted human serum albumin nanoparticle formulation of cabazitaxel for tumor therapy. *International Journal of Nanomedicine* **2019**, *14*, 135-148, https://www.doi.org/10.2147/IJN.S181296.

30. Langer, K.; Balthasar, S.; Vogel, V.; Dinauer, N.; Von Briesen, H.; Schubert, D. Optimization of the preparation process for human serum albumin (HSA) nanoparticles. *International journal of pharmaceutics* **2003**, *257*, 169-180, https://www.doi.org/10.1016/S0378-5173(03)00134-0.
31. Pieper, S.; Onafuye, H.; Mulac, D.; Cinatl Jr, J.; Wass, M.N.; Michaelis, M.; Langer, K. Incorporation of doxorubicin in different polymer nanoparticles and their anticancer activity. *Beilstein journal of nanotechnology* **2019**, *10*, 2062-2072, https://www.doi.org/10.1101/403923.
32. Mattos, A.C.d.; Khalil, N.M.; Mainardes, R.M. Development and validation of an HPLC method for the determination of fluorouracil in polymeric nanoparticles. *Brazilian Journal of Pharmaceutical Sciences* **2013**, *49*, 117-126, https:/doi.org/10.1590/S1984-82502013000100013.
33. Absher, M. Hemocytometer counting. In: *Tissue culture*. Elsevier: **1973**; pp. 395-397, https://doi.org/10.1016/B978-0-12-427150-0.50098-X.
34. Ghafelehbashi, R.; Akbarzadeh, I.; Yaraki, M.T.; Lajevardi, A.; Fatemizadeh, M.; Saremi, L.H. Preparation, physicochemical properties, in vitro evaluation and release behavior of cephalexin-loaded niosomes. *International journal of pharmaceutics* **2019**, *569*, https://doi.org/10.1016/j.ijpharm.2019.118580.
35. Repetto, G.; Del Peso, A.; Zurita, J.L. Neutral red uptake assay for the estimation of cell viability/cytotoxicity. *Nature protocols* **2008**, *3*, https://doi.org/10.1038/nprot.2008.75.
36. Crouch, S.; Kozlowski, R.; Slater, K.; Fletcher, J. The use of ATP bioluminescence as a measure of cell proliferation and cytotoxicity. *Journal of immunological methods* **1993**, *160*, 81-88, https://doi.org/10.1016/0022-1759(93)90011-U.
37. Shandiz, S.S.; Ardestani, M.S.; Irani, S.; Shahbazzadeh, D. Imatinib induces down regulation of Bcl-2 an anti-apoptotic protein in prostate cancer PC-3 cell line. *Adv Stud Biol* **2015**, *7*, 17-27.
38. Kruger, N.J. The Bradford method for protein quantitation. In: *The protein protocols handbook*. Springer: **2009**; pp. 17-24, https://doi.org/10.1385/0-89603-268-X:9.
39. Kielkopf, C.L.; Bauer, W.; Urbatsch, I.L. Bradford assay for determining protein concentration. *Cold Spring Harbor Protocols* **2020**, *2020*, https://doi.org/10.1101/pdb.prot102269.
40. Lombardo, D.; Kiselev, M.A.; Caccamo, M.T. Smart nanoparticles for drug delivery application: development of versatile nanocarrier platforms in biotechnology and nanomedicine. *Journal of Nanomaterials* **2019**, *2019*, https://doi.org/10.1155/2019/3702518.
41. Danaei, M.; Dehghankhold, M.; Ataei, S.; Hasanzadeh Davarani, F.; Javanmard, R.; Dokhani, A.; Khorasani, S.; Mozafari, M. Impact of particle size and polydispersity index on the clinical applications of lipidic nanocarrier systems. *Pharmaceutics* **2018**, *10*, https://doi.org/10.3390/pharmaceutics10020057.
42. Lomis, N.; Westfall, S.; Farahdel, L.; Malhotra, M.; Shum-Tim, D.; Prakash, S. Human serum albumin nanoparticles for use in cancer drug delivery: process optimization and in vitro characterization. *Nanomaterials* **2016**, *6*, https://doi.org/10.3390/nano6060116.
43. Liang, J.; Li, R.; He, Y.; Ling, C.; Wang, Q.; Huang, Y.; Qin, J.; Lu, W.; Wang, J. A novel tumor-targeting treatment strategy uses energy restriction via co-delivery of albendazole and nanosilver. *Nano Research* **2018**, *11*, 4507-4523, https://doi.org/10.1007/s12274-018-2032-x.
44. Borenfreund, E.; Babich, H.; Martin-Alguacil, N. Comparisons of two in vitro cytotoxicity assays—the neutral red (NR) and tetrazolium MTT tests. *Toxicology in vitro* **1988**, *2*, 1-6, https://doi.org/10.1016/0887-2333(88)90030-6.
45. Gough, J.E.; Scotchford, C.A.; Downes, S. Cytotoxicity of glutaraldehyde crosslinked collagen/poly (vinyl alcohol) films is by the mechanism of apoptosis. *Journal of Biomedical Materials Research: An Official Journal of The Society for Biomaterials, The Japanese Society for Biomaterials, and The Australian Society for Biomaterials and the Korean Society for Biomaterials* **2002**, *61*, 121-130, https://doi.org/10.1002/jbm.10145.
46. Rosenblum, D.; Joshi, N.; Tao, W.; Karp, J.M.; Peer, D. Progress and challenges towards targeted delivery of cancer therapeutics. *Nature communications* **2018**, *9*, 1-12, https://doi.org/10.1038/s41467-018-03705-y.
47. Strebhardt, K.; Ullrich, A. Paul Ehrlich's magic bullet concept: 100 years of progress. *Nature Reviews Cancer* **2008**, *8*, 473-480, https://doi.org/10.1038/nrc2394.
48. Zhang, L.; Hou, S.; Mao, S.; Wei, D.; Song, X.; Lu, Y. Uptake of folate-conjugated albumin nanoparticles to the SKOV3 cells. *International journal of pharmaceutics* **2004**, *287*, 155-162, https://doi.org/10.1016/j.ijpharm.2004.08.015.
49. Zhou, J.-D.; Zhang, T.-J.; Xu, Z.-J.; Gu, Y.; Ma, J.-C.; Li, X.-X.; Guo, H.; Wen, X.-M.; Zhang, W.; Yang, L. BCL2 overexpression: clinical implication and biological insights in acute myeloid leukemia. *Diagnostic pathology* **2019**, *14*, https://doi.org/10.1186/s13000-019-0841-1.
50. Yang, J.; Liu, X.; Bhalla, K.; Kim, C.N.; Ibrado, A.M.; Cai, J.; Peng, T.-I.; Jones, D.P.; Wang, X. Prevention of apoptosis by Bcl-2: release of cytochrome c from mitochondria blocked. *Science* **1997**, *275*, 1129-1132, https://doi.org/10.1126/science.275.5303.1129.
51. Singh, S.; Chhipa, R.R.; Vijayakumar, M.V.; Bhat, M.K. DNA damaging drugs-induced down-regulation of Bcl-2 is essential for induction of apoptosis in high-risk HPV-positive HEp-2 and KB cells. *Cancer letters* **2006**, *236*, 213-221, https://doi.org/10.1016/j.canlet.2005.05.024.

52. Macotpet, A.; Suksawat, F.; Sukon, P.; Pimpakdee, K.; Pattarapanwichien, E.; Tangrassameeprasert, R.; Boonsiri, P. Oxidative stress in cancer-bearing dogs assessed by measuring serum malondialdehyde. *BMC veterinary research* **2013**, *9*, https://doi.org/10.1186/1746-6148-9-101.
53. Desideri, E.; Ciccarone, F.; Ciriolo, M.R. Targeting glutathione metabolism: partner in crime in anticancer therapy. *Nutrients* **2019**, *11*, https://doi.org/10.3390/nu11081926.
54. Lu, S.C. Regulation of hepatic glutathione synthesis: current concepts and controversies. *The FASEB Journal* **1999**, *13*, 1169-1183, https://doi.org/10.1096/fasebj.13.10.1169.
55. Dai, X.; Zhou, X.; Liao, C.; Yao, Y.; Yu, Y.; Zhang, S. A nanodrug to combat cisplatin-resistance by protecting cisplatin with p-sulfonatocalix [4] arene and regulating glutathione S-transferases with loaded 5-fluorouracil. *Chemical Communications* **2019**, *55*, 7199-7202, https://doi.org/10.1039/C9CC03012C.
56. Durak, L.; Karaayvaz, M.; Kavutcu, M.; Cimen, M.B.; Kacmaz, M.; Buyukkocak, S.; Ozturk, H.S. Reduced antioxidant defense capacity in myocardial tissue from guinea pigs treated with 5-fluorouracil. *Journal of Toxicology and Environmental Health Part A* **2000**, *59*, 585-589, https://doi.org/10.1080/009841000156709.
57. Rtibi, K.; Selmi, S.; Grami, D.; Amri, M.; Sebai, H.; Marzouki, L. Contribution of oxidative stress in acute intestinal mucositis induced by 5 fluorouracil (5-FU) and its pro-drug capecitabine in rats. *Toxicology mechanisms and methods* **2018**, *28*, 262-267, https://doi.org/10.1080/15376516.2017.1402976.